Inorganic Chemistry
Article

Inorg. Chem. **2010**, *49*, 10057–10066 **10057**
DOI: 10.1021/ic101366z

Iron Complexes for the Catalytic Transfer Hydrogenation of Acetophenone: Steric and Electronic Effects Imposed by Alkyl Substituents at Phosphorus

Paraskevi O. Lagaditis, Alan J. Lough, and Robert H. Morris*

Department of Chemistry, University of Toronto, Toronto, Ontario M5S 3H6, Canada

Received July 8, 2010

A series of iron(II) complexes, *trans*-[Fe(NCMe)$_2$(PR$_2$CH$_2$CH=NCH$_2$CH$_2$N=CHCH$_2$PR$_2$)][BPh$_4$]$_2$ (**5**, R = Cy; **7**, R = *i*Pr; **9**, R = Et) were prepared via the template synthesis in one-pot involving air-stable phosphonium dimers, [*cyclo*-(-PR$_2$CH$_2$CH(OH)−)$_2$](Br)$_2$ (**4**, R = Cy; **6**, R = *i*Pr; **8**, R = Et), KO*t*Bu, [Fe(H$_2$O)$_6$][BF$_4$]$_2$ and ethylenediamine in acetonitrile. In the synthesis of **9**, a methanol/acetonitrile solvent mixture was required; otherwise an intermediate iron bis(tridentate) complex, [Fe(PEt$_2$CH$_2$CH=NCH$_2$CH$_2$NH$_2$)$_2$]$^{2+}$, formed as determined by electrospray ionization mass spectrometry (ESI-MS). The crude iron(II) complexes from a template synthesis with ethylenediamine or (*S*,*S*)-1,2-diphenylethylenediamine are stirred in acetone under a CO atmosphere (∼2 atm) overnight to displace a NCMe ligand; however, in addition to this, bromide displaces an NCMe ligand as well to form a new class of the iron complexes *trans*-[Fe(CO)(Br)(PR$_2$CH$_2$CH=NCHR′CHR′N=CHCH$_2$PR$_2$)]$^+$ (**10** R = Cy, R′ = H; (*S*,*S*)-**11**, R = Cy, R′ = Ph; **12**, R = *i*Pr, R′ = H; (*S*,*S*)-**13**, R = *i*Pr, R′ = Ph; **14**, R = Et, R′ = H; (*S*,*S*)-**15**, R = Et, R′ = Ph). These complexes were isolated in moderate yields (55−84%) as tetraphenylborate salts. Complexes **10**−**15** were tested for the catalytic transfer hydrogenation of acetophenone in basic *iso*-propanol at 25 and 50 °C. The complexes **10**−**13** (where R = Cy or *i*Pr) were inactive while the complexes **14** and (*S*,*S*)-**15** (where R = Et) were active at 25 °C but had better activity at 50 °C. Complex (*S*,*S*)-**15** was higher in activity than complex **14**, achieving turnover frequencies as high as 4100 h^{-1}, conversions of acetophenone to (*R*)-1-phenylethanol as high as 80% and an enantiomeric excess (e.e.) of 50% in the product. As catalysis progressed, the e.e. diminished to as low as 26%.

Introduction

We have entered an "iron-age of chemistry"—the period in which iron catalysts are being found to replace platinum metal catalysts for organic transformations,[1] such as polymerization,[2−6] oxidation,[7−13] or cycloaddition.[14,15] The advantages of iron are its low toxicity, low cost, and high abundance. In the field of cross-coupling, iron catalysts have demonstrated their value as they have high reactivity toward certain substrates (i.e., secondary alkyl halides) which are troublesome to activate for well established palladium and nickel catalysts.[16−22] Since the majority of active iron catalysts for this transformation are generated in situ, they are not practical for large-scale (industrial) applications such that well-defined iron catalysts are sought after.[23,24]

*To whom correspondence should be addressed. E-mail: rmorris@chem.utoronto.ca.

(1) Enthaler, S.; Junge, K.; Beller, M. *Angew. Chem., Int. Ed.* **2008**, *47*, 3317–3321.
(2) Gibson, V. C.; Solan, G. A. *Top. Organomet. Chem.* **2009**, *26*, 107–158.
(3) Müller, G.; Klinga, M.; Leskelä, M.; Rieger, B. *Z. Anorg. Allg. Chem.* **2002**, *628*, 2839–2846.
(4) Kermagoret, A.; Tomicki, F.; Braunstein, P. *Dalton Trans.* **2008**, 2945–2955.
(5) Small, B. L.; Brookhart, M. *Macromolecules* **1999**, *32*, 2120–2130.
(6) Britovsek, G. J. P.; Gibson, V. C.; Mastroianni, S.; Oakes, D. C. H.; Redshaw, C.; Solan, G. A.; White, A. J. P.; Williams, D. J. *Eur. J. Inorg. Chem.* **2001**, 431–437.
(7) Rose, E.; Ren, Q.-Z.; Andrioletti, B. *Chem.—Eur. J.* **2004**, *10*, 224–230.
(8) Yeung, H. L.; Sham, K. C.; Tsang, C. S.; Lau, T. C.; Kwong, H. L. *Chem. Commun.* **2008**, 3801–3803.
(9) Oldenburg, P. D.; Que, J. L. *Catal. Today* **2006**, *117*, 15–21.
(10) Bruijnincx, P. C. A.; Buurmans, I. L. C.; Gosiewska, S.; Moelands, M. A. H.; Lutz, M.; Spek, A. L.; van Koten, G.; Klein Gebbink, R. J. M. *Chem.—Eur. J.* **2008**, *14*, 1228–1237.
(11) Suzuki, K.; Oldenburg, P. D.; Que, L. *Angew. Chem., Int. Ed.* **2008**, *47*, 1887–1889.
(12) Gómez, L.; Garcia-Bosch, I.; Company, A.; Benet-Buchholz, J.; Polo, A.; Sala, X.; Ribas, X.; Costas, M. *Angew. Chem., Int. Ed.* **2009**, *48*, 5720–5723.
(13) Muthupandi, P.; Alamsetti, S. K.; Sekar, G. *Chem. Commun.* **2009**, 3288–3290.
(14) Lai, T. S.; Chan, F. Y.; So, P. K.; Ma, D. L.; Wong, K. Y.; Che, C. M. *Dalton Trans.* **2006**, 4845–4851.
(15) Fürstner, A.; Majima, K.; Martín, R.; Krause, H.; Kattnig, E.; Goddard, R.; Lehmann, C. W. *J. Am. Chem. Soc.* **2008**, *130*, 1992–2004.
(16) Czaplik, W. M.; Mayer, M.; Cvengroš, J.; von Wangelin, A. J. *ChemSusChem.* **2009**, *2*, 396–417.
(17) Bolm, C.; Legros, J.; Le Paih, J.; Zani, L. *Chem. Rev.* **2004**, *104*, 6217–6254.
(18) Liu, L. X. *Curr. Org. Chem.* **2010**, *14*, 1099–1126.
(19) Bauer, E. B. *Curr. Org. Chem.* **2008**, *12*, 1341–1369.
(20) Sherry, B. D.; Fürstner, A. *Acc. Chem. Res.* **2008**, *41*, 1500–1511.
(21) Correa, A.; Mancheño, O. G.; Bolm, C. *Chem. Soc. Rev.* **2008**, *37*, 1108–1117.
(22) Fürstner, A. *Angew. Chem., Int. Ed.* **2009**, *48*, 1364–1367.
(23) Chowdhury, R. R.; Crane, A. K.; Fowler, C.; Kwong, P.; Kozak, C. M. *Chem. Commun.* **2008**, 94–96.
(24) Cahiez, G.; Habiak, V.; Duplais, C.; Moyeux, A. *Angew. Chem., Int. Ed.* **2007**, *46*, 4364–4366.

© 2010 American Chemical Society
Published on Web 10/06/2010

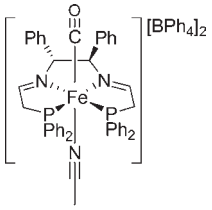

(*R*,*R*)-**1**

Figure 1. Precatalyst for the asymmetric transfer hydrogenation of ketones.

Another breakthrough organic transformation for this metal that has garnered much attention is the asymmetric reduction of prochiral ketones to alcohols.[25−27] This is an important transformation for it allows the synthesis of valuable enantiopure alcohols used for pharmaceuticals, fragrances, and flavors. Current efficient and enantioselective catalysts used in industry for this transformation are based on ruthenium and rhodium complexes.[28−30] Many well-defined iron catalysts have emerged in the literature and have garnered recognition as sustainable alternative catalysts for various modes of reduction. They include Casey et al.'s system for reduction via molecular H_2,[31−33] Chirik and co-workers' catalysts for hydrosilylation,[34−36] and Beller and co-workers'[37−39] for transfer hydrogenation (where the source of hydrogen is *iso*-propanol or $HCOOH/NEt_3$ solution). More recent examples of new iron catalysts for transfer hydrogenation include studies from the groups of Le Floch[40] and Peris and Royo.[41] Many more are yet to come as we continue to discover new ligands that enhance the activity of iron to make it a catalytically competitive metal.

Our work in recent years has focused on the development of iron catalysts specifically for asymmetric transfer hydrogenation.[26] This led to the discovery of the precatalyst (*R*,*R*)-**1**, which when activated with base is the most active and enantioselective iron complex for asymmetric reduction of prochiral ketones to date (Figure 1).[42] Complex (*R*,*R*)-**1** displayed a high activity for the transfer of hydrogen from the *iso*-propanol solvent to acetophenone with a turnover frequency (TOF) of greater than 3600 h^{-1} to give (*S*)-1-phenylethanol in 82% e.e. (where the catalyst/substrate ratio is 1:2000).

Scheme 1. Synthesis of the *trans*-$[Fe(NCMe)_2(P-N-Q-N-P)][BPh_4]_2$ Complexes[a]

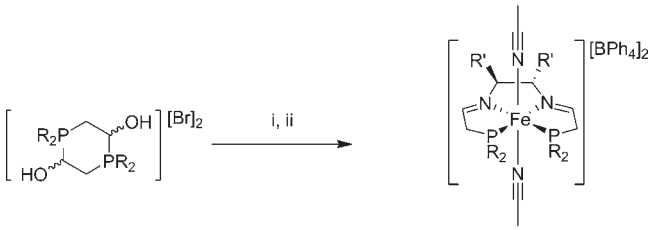

2 R = Ph
4 R = Cy
6 R = *i*Pr
8 R = Et

(*R*,*R*)-**3** R = Ph, R' = Ph
5 R = Cy, R' = H
7 R = *i*Pr, R' = H
9 R = Et, R' = H

[a] (i) 2 KO*t*Bu, 1.5 $[Fe(H_2O)_6][BF_4]_2$, diamine ((*R*,*R*)-dpen for **3**; en for **5**, **7** and **9**); solvent (MeCN/MeOH for **3**, **9** or MeCN for **5** and **7**); T = 25°C for **3**, **5**, **7** or 60°C for **9**; (ii) 2.2 $NaBPh_4$, MeOH.

Precatalyst (*R*,*R*)-**1** was made in a two step procedure that first involved the synthesis of the iron precursor *trans*-$[Fe(NCMe)_2(PPh_2CH_2CH{=}NCHPhCHPhN{=}CHCH_2PPh_2)](BPh_4)_2$ ((*R*,*R*)-**3**) via the template synthesis from a useful phosphino-aldehyde precursor, **2**, in the presence of $[Fe(H_2O)_6][BF_4]_2$ and (*R*,*R*)-1,2-diphenylethylenediamine (dpen) (Scheme 1).[42,43] A template approach is required to synthesize this type of ligand (abbreviated as P−N−Q−N−P) since neither the diamine nor the phosphino-aldehyde contain any conjugation to favor the condensation reaction.[44,45] The optimum reaction solvent for this reaction was found to be a methanol/acetonitrile mixture; if acetonitrile alone is used, a bis(tridentate) iron complex formed which very slowly converted to the desired tetradentate iron product.[43] (*R*,*R*)-**3** was isolated as a tetraphenylborate salt (BPh_4^-) to remove multiple counter-anions, BF_4^- and $FeBr_4^{2-}$ (the latter anion formed in situ), then subjected to a CO atmosphere to replace a NCMe ligand with a CO ligand to make the precatalyst (*R*,*R*)-**1**.

In this report, we examine the effect on the activity of analogues to complex (*R*,*R*)-**1** in the catalytic reduction of ketones by changing the Ph substituents at phosphorus atoms of (*R*,*R*)-**1** to alkyl substituents. A plethora of examples exist in the literature where the change in electronic or sterics of substituents on the ligands (whether it be NHC's, phosphines, etc.) of catalysts completely changed their activity and/or reactivity.[46−56] One famous example is the Grubbs' first

(25) Gaillard, S.; Renaud, J.-L. *ChemSusChem*. **2008**, *1*, 505–509.
(26) Morris, R. H. *Chem. Soc. Rev*. **2009**, 2282–2291.
(27) Chen, J. S.; Chen, L. L.; Xing, Y.; Chen, G.; Shen, W. Y.; Dong, Z. R.; Li, Y. Y.; Gao, J. X. *Acta Chim. Sinica* **2004**, *62*, 1745–1750.
(28) Noyori, R.; Hashiguchi, S. *Acc. Chem. Res*. **1997**, *30*, 97–102.
(29) Ikariya, T.; Blacker, A. J. *Acc. Chem. Res*. **2007**, *40*, 1300–1308.
(30) Wang, C.; Wu, X. F.; Xiao, J. L. *Chem. Asian J*. **2008**, *3*, 1750–1770.
(31) Casey, C. P.; Guan, H. *J. Am. Chem. Soc*. **2007**, *129*, 5816–5817.
(32) Casey, C. P.; Guan, H. *J. Am. Chem. Soc*. **2009**, *131*, 2499–2507.
(33) Bullock, R. M. *Angew. Chem., Int. Ed*. **2007**, *46*, 7360–7363.
(34) Bart, S. C.; Lobkovsky, E.; Chirik, P. J. *J. Am. Chem. Soc*. **2004**, *126*, 13794–13807.
(35) Tondreau, A. M.; Darmon, J. M.; Wile, B. M.; Floyd, S. K.; Lobkovsky, E.; Chirik, P. J. *Organometallics* **2009**, *28*, 3928–3940.
(36) Tondreau, A. M.; Lobkovsky, E.; Chirik, P. J. *Org. Lett*. **2008**, *10*, 2789–2792.
(37) Enthaler, S.; Erre, G.; Tse, M. K.; Junge, K.; Beller, M. *Tetrahedron Lett*. **2006**, *47*, 8095–8099.
(38) Enthaler, S.; Hagemann, B.; Erre, G.; Junge, K.; Beller, M. *Chem. Asian J*. **2006**, *1*, 598–604.
(39) Enthaler, S.; Spilker, B.; Erre, G.; Junge, K.; Tse, M. K.; Beller, M. *Tetrahedron* **2008**, *64*, 3867–3876.
(40) Buchard, A.; Heuclin, H.; Auffrant, A.; Le Goff, X. F.; Le Floch, P. *Dalton Trans*. **2009**, 1659–1667.
(41) Kandepi, V. V. K. M.; Cardoso, J. M. S.; Peris, E.; Royo, B. *Organometallics* **2010**, *29*, 2777–2782.
(42) Mikhailine, A.; Lough, A. J.; Morris, R. H. *J. Am. Chem. Soc*. **2009**, *131*, 1394–1395.
(43) Mikhailine, A. A.; Kim, E.; Dingels, C.; Lough, A. J.; Morris, R. H. *Inorg. Chem*. **2008**, *47*, 6587–6589.
(44) Hoss, R.; Vögtle, F. *Angew. Chem., Int. Ed. Engl*. **1994**, *33*, 375–384.
(45) Busch, D. H.; Stephenson, N. A. *Coord. Chem. Rev*. **1990**, *100*, 119–154.
(46) Kermagoret, A.; Braunstein, P. *Dalton Trans*. **2008**, 822–831.
(47) Page, M. J.; Wagler, J.; Messerle, B. A. *Dalton Trans*. **2009**, 7029–7038.
(48) Namorado, S.; Antunes, M. A.; Veiros, L. F.; Ascenso, J. R.; Duarte, M. T.; Martins, A. M. *Organometallics* **2008**, *27*, 4589–4599.
(49) van der Veen, L. A.; Boele, M. D. K.; Bregman, F. R.; Kamer, P. C. J.; van Leeuwen, P. W. N. M.; Goubitz, K.; Fraanje, J.; Schenk, H.; Bo, C. *J. Am. Chem. Soc*. **1998**, *120*, 11616–11626.
(50) Zuidema, E.; Daura-Oller, E.; Carbó, J. J.; Bo, C.; van Leeuwen, P. W. N. M. *Organometallics* **2007**, *26*, 2234–2242.
(51) Heinicke, J.; Köhler, M.; Peulecke, N.; Keim, W. *J. Catal*. **2004**, *225*, 16–23.
(52) Blaser, H.-U.; Malan, C.; Pugin, B.; Spindler, F.; Steiner, H.; Studer, M. *Adv. Synth. Catal*. **2003**, *345*, 103–151.
(53) Klemps, C.; Payet, E.; Magna, L.; Saussine, L.; Le Goff, X. F.; Le Floch, P. *Chem.—Eur. J*. **2009**, *15*, 8259–8268.
(54) Jahr, H. C.; Nieger, M.; Dötz, K. H. *Chem.—Eur. J*. **2005**, *11*, 5333–5342.
(55) Xie, X.; Zhang, T. Y.; Zhang, Z. *J. Org. Chem*. **2006**, *71*, 6522–6529.
(56) Lane, D. R.; Beavers, C. M.; Olmstead, M. M.; Schore, N. E. *Organometallics* **2009**, *28*, 6789–6797.

generation catalyst in which a balance of the electronics and sterics of the substituents on phosphorus affected the catalytic activity of the catalyst such that PCy_3 proved to be the best phosphine ligand. It was basic enough to stabilize key intermediates in the ring-opening metathesis reactions and yet the Cy substituents were bulky enough to prevent the phosphine ligand from coordinating too strongly.[57−59] In this study, we substitute on phosphorus atoms of the P−N−Q−N−P ligand the alkyl moieties cyclohexyl, *iso*-propyl, and ethyl, explore the catalytic activity of these iron complexes with these new ligands for the transfer hydrogenation of acetophenone, and discuss the effects these changes have on catalytic activity.

Results and Discussion

Synthesis of *trans*-[Fe(NCMe)$_2$(PR$_2$CH$_2$CH=N−Q−N=CHCH$_2$PR$_2$)][BPh$_4$]$_2$ Complexes Where R = Cy, *i*Pr, or Et; Q = −CH$_2$CH$_2$−. We first studied the generality of the template synthesis shown in Scheme 1 when the size of the alkyl group on phosphorus is changed. We recently reported the smooth synthesis of the complex **5** (R = Cy, R′ = H) by the reaction of the phosphonium salt **4** (R = Cy) with KO*t*Bu, ethylenediamine and Fe^{2+} in CH_3CN at room temperature.[60] The reaction of the phosphonium salt **6** (R = *i*Pr)[61] proceeded in a similar fashion to produce complex **7** (R = *i*Pr, R′ = H) with the tetradentate ligand. In these cases no methanol was needed to drive the reaction to completion. However the reactions likely proceed via bis(tridentate) complex intermediates since these have been observed for **2** (R = Ph)[43] and **4** (R = Cy).[60]

The synthesis using the ethyl-substituted phosphonium salt **8** (R = Et)[61] was more challenging since the bis(tridentate) complex [Fe(PEt$_2$CH$_2$CH=NCH$_2$CH$_2$NH$_2$)$_2$]$^{2+}$ formed whether the solvent was acetonitrile or a methanol/acetonitrile mixture. The $^{31}P\{^1H\}$ NMR spectroscopy of the reaction mixtures revealed major and minor species with singlets at 65.5 ppm and 70.7 ppm, respectively. We assign the former signal to the bis(tridentate) complex and the latter to complex **9** containing the tetradentate ligand; the latter is similar to the chemical shift of pure **9** in CD_2Cl_2 (70.5 ppm, see below). This is consistent with the chemical shifts of 63 and 74 ppm observed for the analogous complexes [Fe(PPh$_2$CH$_2$CH=NCH$_2$CH$_2$NH$_2$)$_2$]$^{2+}$ and **2**, respectively.[43] Isolation of the reaction mixtures via salt metathesis with sodium tetraphenylborate ($NaBPh_4$) revealed two masses of interest by electrospray ionization mass spectrometry (ESI-MS): one being for *mer*-[Fe(PEt$_2$CH$_2$CH=NCH$_2$CH$_2$NH$_2$)$_2$]$^{2+}$ (m/z = 403.2) and the other for the free protonated P−N−Q−N−P ligand (m/z = 289.2) from decomposition in the gas phase of the [Fe(NCMe)$_2$(P−N−Q−N−P)]$^{2+}$ complex. Refluxing the dark red reaction mixture in acetonitrile/methanol followed by addition of $NaBPh_4$ to the resulting pale pink solution gave the pure complex **9** (R = Et, R′ = H) as the tetraphenylborate (BPh_4^-) salt. It is unclear why a protic solvent such as methanol is needed to convert the reaction mixtures to the desired iron tetradentate complexes when smaller substituents on phosphorus (Et, Ph) are present while acetonitrile suffices with the bulkier Cy and *i*Pr substituents.

The new complexes **7** and **9** were characterized by NMR spectroscopy, ESI-MS, and X-ray diffraction studies (Figure 2). Pink solutions of the complexes in CD_3CN display singlets in their $^{31}P\{^1H\}$ NMR spectra at 75.9 and 70.8 ppm, respectively. The ESI-MS spectra only show evidence of free tetradentate ligands. The crystal structures reveal a distorted octahedral dicationic complex with *trans* CH_3CN ligands. The P−Fe−P angles are wide and increase as **9** (R = Et) 108.97(3)° < **7** (R = *i*Pr) 112.05(6)° < **5** (R = Cy) 112.92(2)°. This increase in the bond angle as the bulkiness of the substituent increases is not surprising as it follows the trend expected on the basis of Tolman's cone angles.[62] Even though the bond angle widens, there is no lengthening of the Fe−P bond, as is expected since there is no significant electronic difference between the three alkyl substituents.[63]

Thus, template syntheses can be used for all of these substitutions at phosphorus. During the study of the use of such template reactions in the synthesis of the monocarbonyl precatalysts, we discovered that the intermediate step of the precipitation of the *trans*-[Fe(NCMe)$_2$(P−N−Q−N−P)]$^{2+}$ complexes by use of $NaBPh_4$ is unnecessary. Instead they are converted directly to monocarbonyl precatalysts as described below. However multiple counteranions ($FeBr_4^{2-}$ and BF_4^-) are carried over to the next step of the synthesis and this results in the surprising formation of carbonyl bromide complexes [Fe(CO)(Br)(P−N−Q−N−P)]$^+$ (Scheme 2).

Acetonitrile/Carbon Monoxide Exchange Reactions. After following the template procedure as described in step (i) of Scheme 1, the solvent was evaporated, acetone was added to the residue, and the mixture stirred overnight under CO (∼2 atm). The red-pink mixtures turned to brown-yellow, a good indication of a successful CO ligand substitution reaction. The ^1H and $^{31}P\{^1H\}$ NMR spectra of the yellow solids obtained after the salt metathesis with $NaBPh_4$ revealed full conversion to complexes **10**−**15** in 55−84% overall yield. The $^{31}P\{^1H\}$ NMR spectra in CD_2Cl_2 of achiral complexes **10**, **12**, and **14** (where Q = −CH$_2$CH$_2$−) revealed a singlet while the spectra of complexes (*S*,*S*)-**11**, (*S*,*S*)-**13** and (*S*,*S*)-**15** (where Q = (*S*,*S*)-CH(Ph)CH(Ph)−) revealed two doublets. In the ^1H NMR spectra, the most distinguishable feature which further supported evidence of the bromide *trans* to carbonyl geometry was by inspection of the −CH$_2$P protons (Figure 3). These protons become diastereotopic since they are in different environments, where one H is on the same side of the tetradentate ligand plane as the CO ligand while the other is on the side with the bromide ligand. The $^{13}C\{^1H\}$ NMR spectra are consistent with the structures shown in Scheme 2; however, the resonance for the CO ligand was too weak to be detected.

IR spectra of complexes **10**−**15** revealed one CO stretch and no CN stretch from coordinated acetonitrile (Table 1).

(57) Dias, E. L.; Nguyen, S. T.; Grubbs, R. H. *J. Am. Chem. Soc.* **1997**, *119*, 3887–3897.
(58) Grubbs, R. H. *Tetrahedron* **2004**, *60*, 7117–7140.
(59) Nguyen, S. T.; Grubbs, R. H.; Ziller, J. W. *J. Am. Chem. Soc.* **1993**, *115*, 9858–9859.
(60) Lagaditis, P. O.; Mikhailine, A. A.; Lough, A. J.; Morris, R. H. *Inorg. Chem.* **2010**, *49*, 1094–1102.
(61) Mikhailine, A. A.; Lagaditis, P. O.; Sues, P. E.; Lough, A. J.; Morris, R. H. *J. Organomet. Chem.* **2010**, *695*, 1824–1830.
(62) Tolman, C. A. *Chem. Rev.* **1977**, *77*, 313–348.
(63) Liu, H. Y.; Eriks, K.; Prock, A.; Giering, W. P. *Organometallics* **1990**, *9*, 1758–1766.

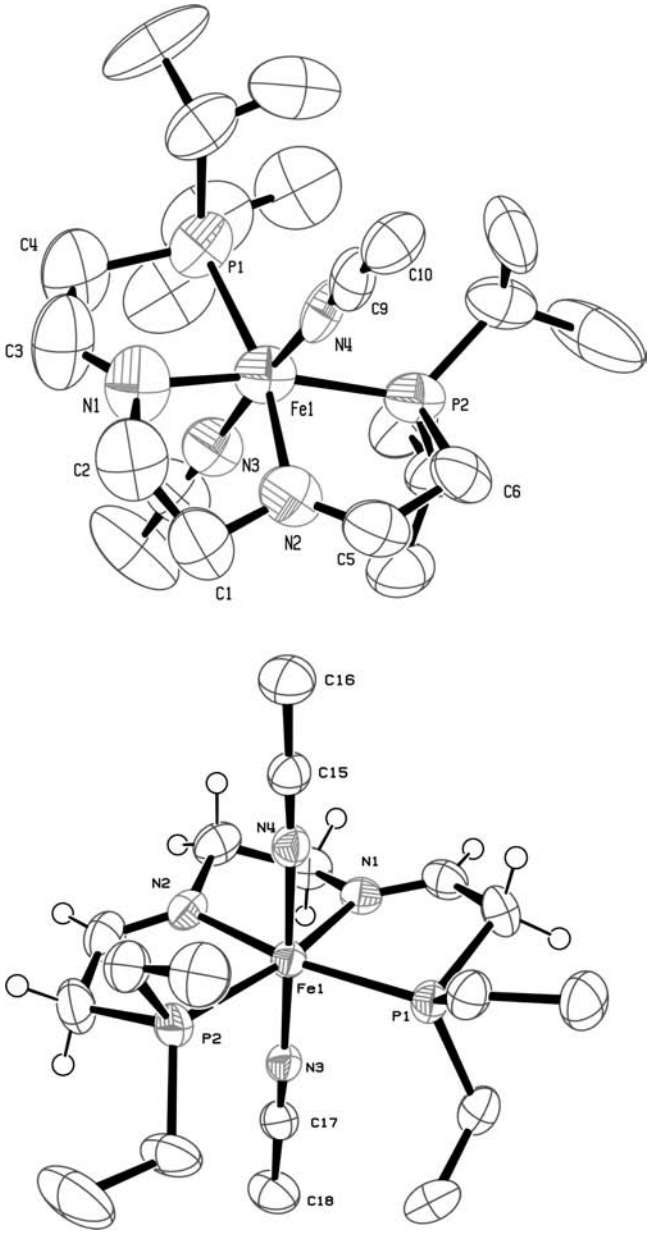

Figure 2. ORTEP plot (thermal ellipsoids at 50% probability) of the X-ray crystal structures of **7** (top) and **9** (bottom). The BPh_4^- counteranions, most hydrogen atoms, and disordered molecules were removed for clarity (see Supporting Information). Selected bond lengths (Å) and angles (deg): for **7**, Fe(1)−N(1), 1.962(4); Fe(1)−N(3), 1.910(5); Fe(1)−P(1), 2.281(2); Fe(1)−P(2), 2.275(2); N(1)−Fe(1)−N(2), 82.8(2); N(3)−Fe(1)−N(4), 173.4(5); P(1)−Fe(1)−P(2), 112.05(6); for **9**, Fe(1)−N(1), 1.958(2); Fe(1)−N(3), 1.921(2); Fe(1)−P(1), 2.225(8); Fe(1)−P(2), 2.215(8); N(1)−Fe(1)−N(2), 83.37(1); N(3)−Fe(1)−N(4), 177.76(1); P(1)−Fe(1)−P(2), 108.97(3).

As expected, the CO stretch decreases in wavenumber as the substituent on phosphorus increases in donicity. Thus, the more donating Cy group causes the lowest CO wavenumbers. The substituent on the diamine has little effect on the electronics at the metal since the CO wavenumber changes little, at least on going from **10** to (*S*,*S*)-**11** and **14** to (*S*,*S*)-**15**.

Once crystals suitable for X-ray diffraction were grown, we found there was no MeCN ligand coordinated to iron but rather a bromide ligand (Figure 4). Complexes **10**, (*S*,*S*)-**13**, **14**, and (*S*,*S*)-**15** were characterized by X-ray diffraction

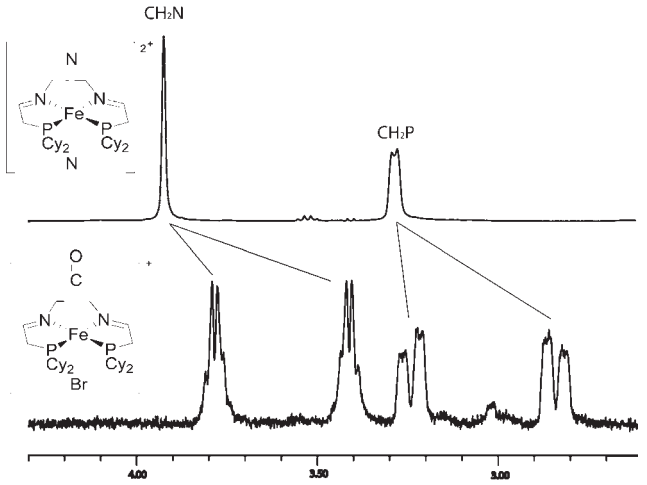

Figure 3. ^1H NMR (CD_2Cl_2) spectra of complexes **5** (top) and **10** (bottom) showing the CH_2N and CH_2P resonances which are homotopic in **5** but diastereotopic in **10**.

Scheme 2. Synthesis of *trans*-[Fe(CO)(Br)(P−N−Q−N−P)][BPh_4] Complexes[a]

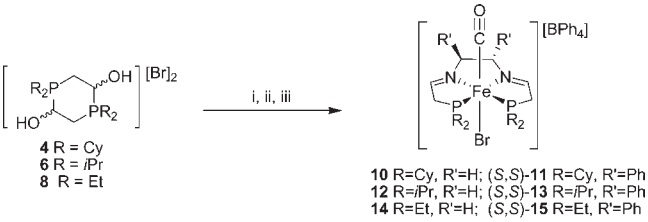

4 R = Cy
6 R = *i*Pr
8 R = Et

10 R=Cy, R'=H; (*S*,*S*)-**11** R=Cy, R'=Ph
12 R=*i*Pr, R'=H; (*S*,*S*)-**13** R=*i*Pr, R'=Ph
14 R=Et, R'=H; (*S*,*S*)-**15** R=Et, R'=Ph

[a] (i) 2 KO*t*Bu, 1.5 $[Fe(H_2O)_6][BF_4]_2$, ethylenediamine, or (*S*,*S*)-1,2-diphenylethylenediamine, conditions as in Scheme 1, then evaporate; (ii) CO (∼2 atm), acetone; (iii) 1.1 $NaBPh_4$, MeOH.

Table 1. Infrared Data for Complexes **10**−**15**

compound	ν(C≡O), cm^{-1} (KBr pellet)
(*R*-*R*)-**1**	2001
10	1948
(*S*,*S*)-**11**	1945
12	1948
(*S*,*S*)-**13**	1956
14	1951
(*S*,*S*)-**15**	1951

studies, bond lengths and angles of interest are summarized in Table 2, and selected crystal data in Table 3. All of the aforementioned complexes have a pseudo trans-octahedral geometry. The most noticeable feature is the large P−Fe−P bond angles as in the $[Fe(NCMe)_2(P-N-Q-N-P)]^{2+}$ complexes (above). This is due primarily to the constrained geometry of the tetradentate ligands that form three 5,5,5- membered rings with the metal ion. There is also a steric effect from the alkyl substituents at the phosphorus atoms in which **10** (R = Cy) with the bulkiest substituents has the largest bond angle (112.73(3)°) followed sequentially by (*S*,*S*)-**13**, **14**, and (*S*,*S*)-**15**. There is not a significant difference between the P−Fe−P bond angles of the $[Fe(CO)(Br)(P-N-Q-N-P)]^+$ and the $[Fe(NCMe)_2(P-N-Q-N-P)]^{2+}$ complexes (**5** vs **10**, **7** vs **13**, and **9** vs **14**). Hence, neither of the axial ligands has an effect on the P−Fe−P bond angle and thus this angle is directly related

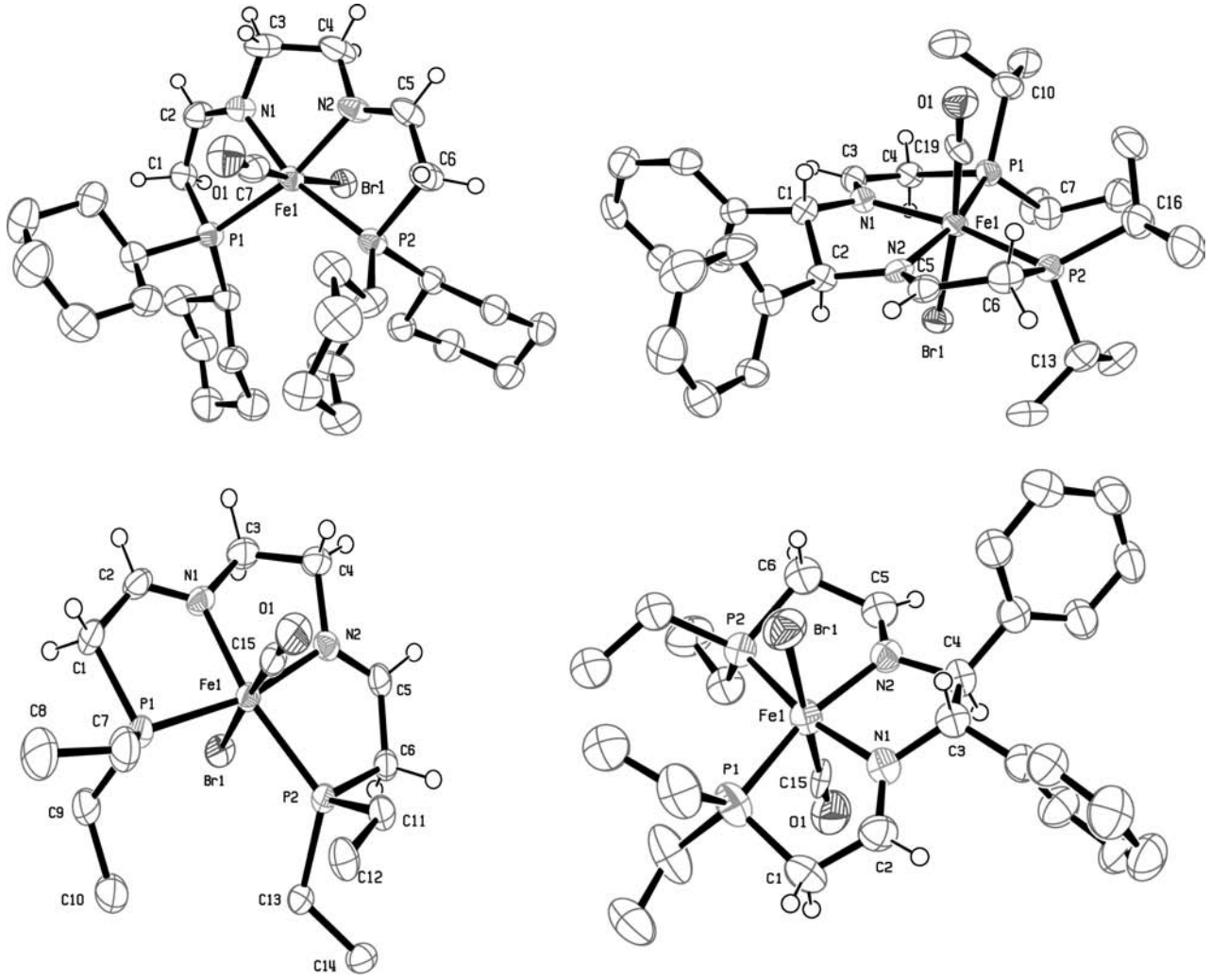

Figure 4. ORTEP plot (thermal ellipsoids at 50% probability) of the X-ray crystal structures of **10** (top, left), (*S*,*S*)-**13** (top, right), **14** (bottom, left) and (*S*,*S*)-**15** (bottom, right). The counteranions, most hydrogen atoms, and any other disordered molecules were removed for clarity (see Supporting Information).

to the substituents at phosphorus as well as the geometry of the 5,5,5-membered rings.

The preferred formation of the complexes with CO trans to Br rather than to acetonitrile is explained by the fact that Br is an anionic σ- and π-donor ligand while acetonitrile is a neutral σ-donor and π-acceptor ligand. This makes Br a more suitable ligand when trans to CO, a π-acceptor. The π-donating nature of the Br ligand in complexes **10**−**15** is evident from the IR spectra. The IR $\nu_{C\equiv O}$ absorption peaks are lowered to the range of 1940−1960 cm^{-1}, in comparison with complex (*R*,*R*)-**1** whose $\nu_{C\equiv O}$ absorption peak is at 2001 cm^{-1} (Table 1). The $\nu_{C\equiv O}$ peaks of complexes **10**−**15** fall in the range for other known iron complexes that also have a π-donating halide coordinated trans to a CO ligand.[64−67] Furthermore, the preferred formation of CO trans to Br is an advantage for synthetic considerations. The CO exchange reaction to form complex (*R*,*R*)-**1** is more tedious as the acetone solvent must be replenished at least once to completely remove all the dissociated acetonitrile and hence to drive the substitution reaction to completion; otherwise trace amounts of (*R*,*R*)-**3** remained as determined by $^{31}P\{^1H\}$ NMR spectroscopy. Nevertheless, these newly synthesized complexes with carbonyl and bromide as ligands are not inert toward acetonitrile substitution when the isolated solids are taken up in acetonitrile. For example, a $^{31}P\{^1H\}$ NMR spectrum of

Table 2. Selected Bond Lengths (Å) and Angles (deg) for **10**, (*S*,*S*)-**13**, **14**, and (*S*,*S*)-**15**

	10	(*S*,*S*)-**13**	**14**	(*S*,*S*)-**15**
Bond Lengths (Å)				
Fe−Br	2.487 (8)	2.508 (7)	2.487 (6)	2.422 (1)
Fe−P(1)	2.284 (8)	2.259 (1)	2.236 (1)	2.219 (2)
Fe−N(1)	1.980 (2)	1.970 (3)	1.974 (3)	1.958 (4)
Fe−C[a]	1.731 (5)	1.757 (5)	1.739 (4)	1.814 (9)
C[a]-O(1)	1.165 (8)	1.115 (5)	1.153 (4)	1.162 (1)
Bond Angles (deg)				
P(1)−Fe-P(2)	112.72 (3)	111.73 (5)	110.66 (4)	108.23 (5)
N(1)−Fe−N(2)	81.83 (1)	82.55 (2)	82.43 (1)	83.01 (2)

[a] **10**: C(7); (*S*,*S*)-**13**: C(19); **14**, (*S*,*S*)-**15**: C(15).

(64) Venturi, C.; Bellachioma, G.; Cardaci, G.; Macchioni, A. *Inorg. Chim. Acta* **2004**, *357*, 3712–3720.
(65) Gao, Y.; Holah, D. G.; Hughes, A. N.; Spivak, G. J.; Havighurst, M. D.; Magnuson, V. R.; Polyakov, V. *Polyhedron* **1997**, *16*, 2797–2807.
(66) Bellerby, J. M.; Mays, M. J.; Sears, P. L. *J. Chem. Soc., Dalton Trans.* **1976**, 1232–1236.
(67) Albertin, G.; Baldan, D.; Bordignon, E. *J. Chem. Soc., Dalton Trans.* **1986**, 329–332.

Table 3. Selected Crystal Data, Data Collection, and Refinement Parameters for **7**, **9**, **10**, (*S*,*S*)-**13**, **14**, and (*S*,*S*)-**15**

	7	**9**·CH_2Cl_2	**10**·THF	(*S*,*S*)-**13**	**14**	(*S*,*S*)-**15**
empirical formula	$C_{70}H_{84}B_2FeN_4P_2$	$C_{67}H_{78}B_2Cl_2FeN_4P_2$	$C_{59}H_{82}BBrFeN_2O_2P_2$	$C_{55}H_{66}BBrFeN_2OP_2$	$C_{39}H_{50}BbrFeN_2OP_2$	$C_{51}H_{58}BBrFeN_2OP_2$
FW	1120.82	1149.64	1059.78	979.61	771.32	923.50
lattice type	monoclinic	monoclinic	monoclinic	orthorhombic	monoclinic	orthorhombic
space group	$P2_1/n$	$P2_1/n$	$P2_1/c$	$P2_12_12_1$	$P2_1/c$	$P2_12_12_1$
T, K	150(1)	150(1)	150(1)	150(1)	150(1)	150(1)
a, Å	13.0271(2)	23.6919(6)	11.1247(2)	12.8978(3)	25.8207(5)	12.4275(3)
b, Å	26.9138(7)	11.9363(2)	21.3615(3)	16.6086(3)	29.1920(6)	15.4890(5)
c, Å	17.7660(4)	24.7617(6)	25.1343(5)	23.5406(5)	10.1299(2)	24.0452(7)
α, deg	90	90	90	90	90	90
β, deg	91.0020(1)	118.3990(8)	92.2340(9)	90	98.109(1)	90
γ, deg	90	90	90	90	90	90
V, Å^3	6228.0(2)	6159.8(2)	5968.38(2)	5042.74(2)	7559.1(3)	4628.4(2)
Z	4	4	4	4	8	4
ρ_{calc}/Mg m^{-3}	1.195	1.240	1.179	1.290	1.356	1.325
μ(Mo, Kα), mm^{-1}	0.338	0.427	1.015	1.195	1.574	1.297
F(000)	2392	2432	2248	2056	3216	1928
cryst size, mm^3	0.15 × 0.15 × 0.10	0.30 × 0.20 × 0.16	0.20 × 0.15 × 0.14	0.20 × 0.20 × 0.15	0.36 × 0.12 × 0.04	0.25 × 0.18 × 0.09
range θ collected, deg	2.75 to 25.00	2.59 to 27.51	2.58 to 27.48	2.60 to 27.54	2.63 to 27.47	2.63 to 26.72
reflns collected/unique	40634/10946	48792/14056	38865/13607	42429/11494	60298/17278	34619/9506
abs cor	semiempirical from equivalents					
max and min transmn coeff.	0.976 and 0.804	0.966 and 0.832	0.913 and 0.867	0.838 and 0.776	0.982 and 0.684	0.890 and 0.771
goodness of fit	1.044	1.028	1.031	1.022	0.972	1.036
$R_1(I > 2\sigma(I))$[a]	0.0828	0.0560	0.0550	0.0553	0.0545	0.0556
wR_2 (all data)[a]	0.2573	0.1589	0.1410	0.1183	0.1286	0.1203
peak and hole, e Å^{-3}	1.564 and −0.637	0.959 and −0.641	0.523 and −0.400	0.605 and −0.535	0.540 and −0.674	0.313 and −0.326

[a] Definition of R indices: $R_1 = \sum(F_O - F_C)/\sum(F_O)$; $wR_2 = [\sum[w(F_O^2 - F_C^2)^2]/[\sum[w(F_O^2)^2]]^{1/2}$.

the reaction in which complex **12** was taken up in acetonitrile-d_3 revealed two species, a singlet at 76.0 ppm for **7** and a singlet at 77.9 ppm for **12**. In addition, when (*S*,*S*)-**15** was dissolved in acetonitrile-d_3, the spectrum showed after 1 day the presence of two species, a singlet at 69.4 ppm and a doublet of doublets centered at 66.9 ppm for the complexes *trans*-$[Fe(NCCH_3)_2(PEt_2CH_2CH{=}NCHPh\text{-})_2]^{2+}$ and (*S*,*S*)-**15**, respectively.

Transfer Hydrogenation of Ketones. We have previously shown that the iron bis(acetonitrile) complex (*R*,*R*)-**3** was inactive for the transfer hydrogenation of ketones in basic *iso*-propanol. Complexes **5**, **7**, and **9** were also tested, and they too were inactive for the transfer hydrogenation of acetophenone in the same conditions.[42] As demonstrated by (*R*,*R*)-**1**, for reasons unknown yet, a carbonyl ligand is necessary to make these types of iron complexes active transfer hydrogenation catalysts. Hence, complexes **10**−**15** were tested for the transfer hydrogenation of acetophenone to 1-phenylethanol in basic *iso*-propanol. To our surprise, complexes **10**−**13** were inactive for transfer hydrogenation at room temperature and even at 50 °C. Complexes **14** and (*S*,*S*)-**15**, on the other hand, showed activity for the transfer hydrogenation of acetophenone at room temperature but better activity at 50 °C (Table 4). Complexes **14** and (*S*,*S*)-**15** were inactive in the absence of base, a common observation with analogous iron complexes[42,68,69] and well established ruthenium-based complexes for transfer hydrogenation.[70−72]

At 25 °C, complex **14** catalyzed the reduction of acetophenone to 1-phenylethanol to 15% conversion in 1 h (Table 4, entry 1) and only to a maximum of 20% conversion after overnight; whereas, a maximum conversion of 70% was achieved after 12 h at 50 °C. At a higher substrate loading, complex **14** led to a maximum 50% conversion of acetophenone to 1-phenylethanol after 1 h at 50 °C (Table 4, entry 3). In general, complex (*S*,*S*)-**15** is a better catalyst than **14** in the reduction of acetophenone (i.e., Table 4, entry 6 vs entry 3; Figure 5) in which there is a substantial increase in the TOF (h^{-1}). The activity of the catalyst does not appear to be affected by the choice of base since the use of sodium *iso*-propoxide or potassium hydroxide in the same catalyst/base ratio of 1/8 gave similar conversions and TOF as with potassium *tert*-butoxide (Table 4, entries 6−8).

The enantioselectivity in the reduction of acetophenone catalyzed by (*S*,*S*)-**15** (e.e. = 55%) was much lower than that of complex (*R*,*R*)-**1** (e.e. = 82%). Hence, it appears as though some degree of rigid steric bulk is required at the phosphorus to maintain high enantioselectivity. At 25 °C, the enantioselectivity of (*S*,*S*)-**15** for (*R*)-1-phenylethanol was fairly constant such that the e.e. degraded from 57 to 44% when the reaction mixture was left stirring for 12 h. At 50 °C, however, the alcohol product racemized early in the catalysis such that only 26−29% e.e. was observed at 1 h (Table 4, entry 10 and 11). Racemization of the alcohol product has been observed previously in the transfer hydrogenation using complex (*R*,*R*)-**1**.[42] An increase in the precatalyst loading caused an increase in e.e. as long as the product is analyzed as soon as the equilibrium is reached (entry 4 vs 6).

Figure 5 depicts the catalytic behavior of **14** and (*S*,*S*)-**15** where the catalyst/base/substrate ratio is 1/8/500. In all cases, no induction period was observed and rapid conversion was observed in the first 10 min; afterward, the catalysis began to plateau. This is a strong indication the

(68) Sui-Seng, C.; Freutel, F.; Lough, A. J.; Morris, R. H. *Angew. Chem., Int. Ed.* **2008**, *47*, 940–943.
(69) Meyer, N.; Lough, A. J.; Morris, R. H. *Chem.—Eur. J.* **2009**, *15*, 5605–5610.
(70) Gao, J.-X.; Ikariya, T.; Noyori, R. *Organometallics* **1996**, *15*, 1087–1089.
(71) Gao, J.-x.; Xu, P.-p.; Yi, X.-d.; Yang, C.-b.; Zhang, H.; Cheng, S.-h.; Wan, H.-l.; Tsai, K.-r.; Ikariya, T. *J. Mol. Catal. A: Chem.* **1999**, *147*, 105–111.
(72) Gao, J.-X.; Zhang, H.; Yi, X.-D.; Xu, P.-P.; Tang, C.-L.; Wan, H.-L.; Tsai, K.-R.; Ikariya, T. *Chirality* **2000**, *12*, 383–388.

Table 4. Catalytic Transfer Hydrogenation of Acetophenone to 1-Phenylethanol in *iso*-Propanol

entry/ complex	C/B/S[a] ratio	temperature (°C)	conversion[b]/ 2 min (%)	conversion[b]/ 10 min (%)	conversion[b]/ 60 min (%)	e.e. (%)[c] 2 min/ 60 min	TOF[d] (h^{-1})
1/**14**	1/8/200	25		10	15		119
2/**14**	1/8/200	50	21	46	66		735
3/**14**	1/8/500	50	13	34	47		1458
4/**15**	1/8/50	50	92			60/-	
5/**15**	1/8/100	50	86	91		54/24	
6/**15**	1/8/200	50	66	89		55/47[e]	2421
7/**15**[f]	1/8/200	50	62	90		57/47[e]	2341
8/**15**[h]	1/8/200	50	54	90		58/47[e]	2245
9/**15**	1/8/500	25	6	19	35	57/51	563
10/**15**	1/8/500	50	29	72	81	56/26	4171
11/**15**	1/8/1000	50	5	25	50	53/29	1551

[a] C/B/S: catalyst/base/substrate. [b] Conversions were determined by GC and were reported as an average of two runs. [c] enantiomeric excess in (*R*)-1-phenylethanol. [d] TOF calculated from slope of initial linear portion of catalysis. [e] %e.e. at 2 min/10 min. [f] NaO*i*Pr used as base. [h] KOH used as base.

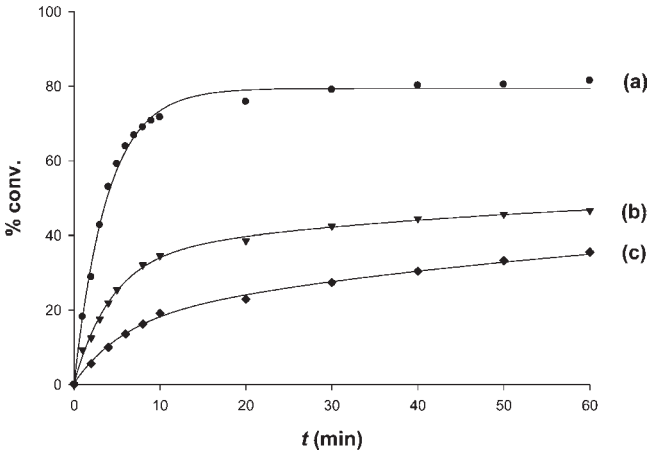

Figure 5. Catalytic transfer hydrogenation of acetophenone to 1-phenylethanol in the presence of **14** or (*S*,*S*)-**15**, potassium *tert*-butoxide, and *iso*-propanol (6 mL). C/B/S = 1/8/500. (a) precatalyst: (*S*,*S*)-**15**; T = 50 °C; (b) precatalyst: **14**; T = 50 °C; (c) precatalyst: (*S*,*S*)-**15**; T = 25 °C.

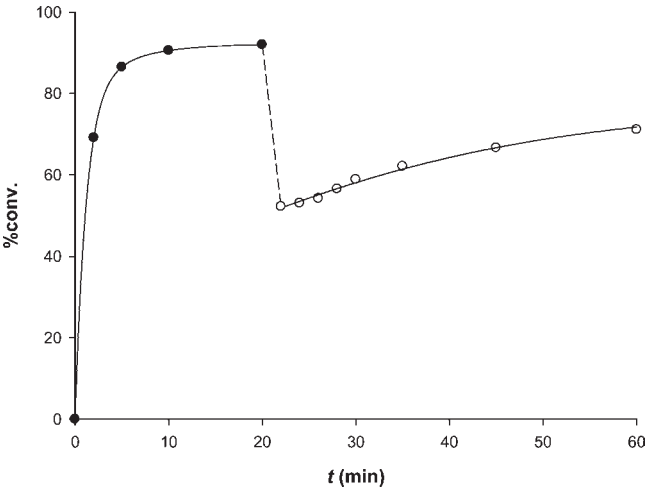

Figure 6. Second addition of acetophenone (260 mg, C/S = 1/200) after 20 min of transfer hydrogenation of acetophenone in the presence of (*S*,*S*)-**15**, potassium *tert*-butoxide and *iso*-propanol (6 mL) at 50 °C (C/B/S = 1/8/200).

active catalyst slowly deactivates during the course of the catalysis.

To test this, additional acetophenone (200 equiv) was added after 20 min to a catalytic reaction mixture that had a catalyst/substrate ratio of 1/200 (Figure 6). Thus, upon the second addition of acetophenone, the catalyst displayed different catalytic behavior. The initial sharp, rapid increase in catalysis was not observed; rather it was a slow and steady increase such that it took more than twice the amount of time to achieve almost the same concentration of 1-phenylethanol. We attribute this to decomposition of the active species during catalysis.

To further demonstrate the catalyst decomposition process, additional precatalyst was added during the course of catalysis (Figure 7). In the case of the catalyst to ketone ratio of 1:500 (Figure 7, a), additional precatalyst was added after 60 min; this had a small effect which indicated that the initial (*S*,*S*)-**15** to ketone loading of 1/500 allowed for an almost complete approach to equilibrium before catalyst decomposition. However, in the case of the catalyst to ketone ratio of 1:1000 (Figure 7, b) catalysis resumed after an additional 10 mg of catalyst was added after 60 min. A third addition of (*S*,*S*)-**15** had little effect on the conversion, indicating that equilibrium was reached. These experiments provide clear evidence for the decomposition of the catalyst during catalysis.

In spite of the activity of complex **14** and the increased activity of complex (*S*,*S*)-**15** at 50 °C, they are less active than complex (*R*,*R*)-**1**. At a catalyst/substrate ratio of 1/500, complex (*S*,*S*)-**15** displayed a TOF of 4100 h^{-1} at 50 °C, while both complex (*R*,*R*)-**1** and the bromo variant *trans*-[Fe(Br)(CO)($PPh_2CH_2CH{=}NCH_2CH_2N{=}CH$-$CH_2PPh_2$)]$^+$,[75] at similar concentrations have a TOF of 3600 h^{-1} at the lower temperature of 22 °C. The higher activity of the PPh_2-substituted complexes is clearly an electronic effect in which phenyl substituents at phosphorus are necessary to increase the activity of these tetradentate iron complexes.

An electronic effect is also evident by the comparison of the catalytic activities between complexes **14** and (*S*,*S*)-**15** (Figure 5, a and b). The phenyl groups on the NN-linker of the ligand of (*S*,*S*)-**15**, not conjugated to the tetradentate

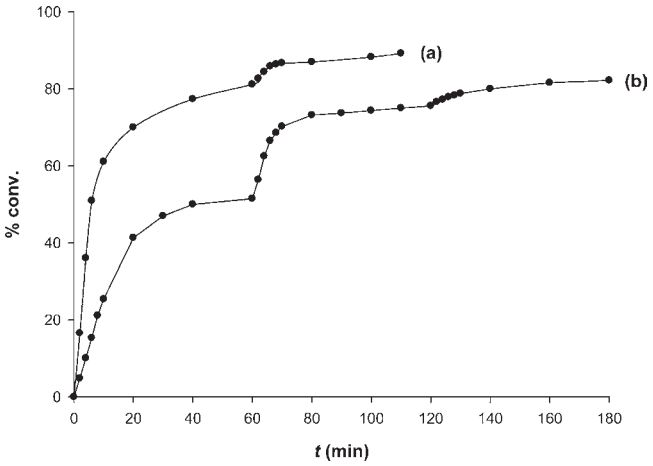

Figure 7. Addition of 10 mg of (*S*,*S*)-**15** to catalytic transfer hydrogenation reactions at 50 °C in the presence of potassium *tert*-butoxide. (a) Second addition added after 60 min (initial C/S = 1/500). (b) Second addition added after 60 min, third addition added after 120 min (initial C/S = 1/1000).

ligand, increased the catalytic activity for the reduction of acetophenone. However, this electronic withdrawing effect had a smaller effect such that catalytic activity is still inferior to (*R*,*R*)-**1**. The difference in the NN-linker had no effect in increasing the activity of (*S*,*S*)-**11** and (*S*,*S*)-**13** over **10** and **12**, respectively, indicating the substituents at the phosphorus have a dominant role in the activity of these iron complexes for transfer hydrogenation of ketones. We also believe steric factors are involved which make complexes **10**−**13** inactive for transfer hydrogenation but make complexes **14** and (*S*,*S*)-**15** active. The Cy or *i*Pr groups may block a key site on the P−N−Q−N−P ligand backbone; mechanistic investigations of the Noyori catalyst system $RuCl_2$(P−N−N−P) and its analogues have shown that the P−N−N−P ligand system is not an ancillary ligand and is involved in the catalytic cycle—this mode of action has been coined as "ligand-metal bifunctional catalysis".[73,74] Hence, this blockage created by those substituents may prevent either *iso*-propanol and/or the substrate (acetophenone) to interact with the P−N−Q−N−P ligand and iron metal center of the active complex.

This rationale also leads to an additional possibility in which dissociation of a phosphine donor atom of the ligand from iron is required in the catalytic cycle. Since electron donating alkyl substituents render phosphines more basic, the ligands would be less likely to dissociate. Even though this latter scenario appears to explain the difference in catalytic activity between complex (*R*,*R*)-**1** and complexes **10**−**15**, we are not in favor of it because it is insufficient to explain the difference between the inactivity of complexes **10**−**13** and the activity of complexes **14**−**15**.

These theories are still speculation as the mechanism is not known. Density functional theory (DFT) analysis of the mechanism is currently under investigation by our group.

(73) Clapham, S. E.; Hadzovic, A.; Morris, R. H. *Coord. Chem. Rev.* **2004**, *248*, 2201–2237.
(74) Rautenstrauch, V.; Hoang-Cong, X.; Churlaud, R.; Abdur-Rashid, K.; Morris, R. H. *Chem.—Eur. J.* **2003**, *9*, 4954–4967.
(75) Mikhailine, A. A., Morris, R. H. *Inorg. Chem.* submitted for publication, 2010.

Conclusion

We have made a series of new iron complexes, [Fe(CO)(Br)-(P−N−Q−N−P)][BPh_4] for the transfer hydrogenation of ketones that feature alkyl substituents (Cy, *i*Pr, Et) at phosphorus. They are first made as bis-acetonitrile iron complexes in a facile one-pot template reaction and then subjected to a CO atmosphere; thereafter, the complexes are isolated as BPh_4 salts in moderate to good yields. The complexes that contained Cy or *i*Pr substituents (**10**−**13**) at phosphorus were inactive while those with Et substituents (**14** and (*S*,*S*)-**15**) were active for the catalytic reduction of acetophenone. In addition, complex (*S*,*S*)-**15**, with Ph substituents on the NN-linker backbone, displayed higher activity than complex **14**. Despite the activity of complexes **14** and (*S*,*S*)-**15**, they are less active than complex (*R*,*R*)-**1**. This observation clearly indicates that electron-withdrawing groups are necessary for the high enzymatic-like activity of complex (*R*,*R*)-**1**. Furthermore, the inactivity of complexes **10**−**13**, indicate that there cannot be too much steric bulk at the phosphorus donor atoms of the ligand. Yet the poor enantioselectivity of complex (*S*,*S*)-**15** indicated there some degree of steric bulk is required; thus, this report showed by comparison that the Ph groups on the phosphorus atoms of the ligand of complex (*R*,*R*)-**1** provide a fine balance between sterics and electronics.

Experimental Section

General Comments. All procedures and manipulations involving air-sensitive materials were performed under an argon or nitrogen atmosphere using Schlenk techniques or a glovebox with N_2(g). Solvents were degassed and dried using standard procedures prior to all manipulations and reactions. Deuterated solvents were purchased from Cambridge Isotope Laboratories, degassed and dried over activated molecular sieves prior to use. Phosphonium dimers **4**, **6**, and **8**, were synthesized following a literature procedure.[60,61] All other reagents used were purchased from commercial sources and utilized without further purifications. NMR spectra were recorded at ambient temperature and pressure using Varian Gemini 400 MHz [^{1}H (400 MHz), ^{13}C{^{1}H} (100 MHz) and ^{31}P{^{1}H} (161 MHz)]. The ^{31}P NMR spectra were referenced to 85% H_3PO_4 (0 ppm). The elemental analyses were performed at the Department of Chemistry, University of Toronto, on a Perkin-Elmer 2400 CHN elemental analyzer. Some complexes gave inconsistent carbon analyses but acceptable hydrogen and nitrogen contents; we attribute it as a combustion problem due to tetraphenylborate.[76]

Precursor Solution A. A vial was charged with **4** (100 mg, 0.156 mmol), KO*t*Bu (35 mg, 0.311 mmol), and CH_3CN (5 mL). After stirring for 5 min, [Fe(H_2O)$_6$][BF_4]$_2$ (79 mg, 0.234 mmol) in CH_3CN (2 mL) was added to the white slurry. The solution turned gray-yellow after 5 min.

***trans*-[Fe(CO)(Br)($PCy_2CH_2CH{=}NCH_2CH_2N{=}CHCH_2PCy_2$)][$BPh_4$] (10).** To precursor solution **A**, ethylenediamine (0.17 mL from a stock solution of 200 mg in 4 mL of CH_3CN) was added. The mixture turned pink immediately. After the reaction had gone to completion overnight, the mixture was filtered through a pad of Celite to remove a gray-white precipitate. Solvent was removed under reduced pressure to give a red-pink residue, which was then dissolved in acetone (6 mL) and stirred overnight under CO (∼ 2 atm). Acetone solvent was removed under pressure, taken up in MeOH (1.5 mL), and added to a solution of $NaBPh_4$ (80 mg, 0.234 mmol) in MeOH (1 mL) to cause precipitation of a yellow solid. The solid was filtered and washed with MeOH (2 × 1 mL) and dried under vacuum. Yield: 80%

(76) Marco, A.; Compano, R.; Rubio, R.; Casals, I. *Microchim. Acta* **2003**, *142*, 13–19.

(123 mg). Single crystals suitable for an X-ray diffraction study were obtained by slow diffusion of hexanes into tetrahydrofuran (THF). ^{1}H NMR (400 MHz, CD_2Cl_2) δ: 1.20−1.39 (m, *H*Cy), 2.50 (br. m, 2H, *H*CyP) 2.86 (dd, J_{HP} = 19.0 Hz, 2H, H_2CP), 3.27 (dd, J_{HP} = 20.0 Hz, 2H, H_2CP), 3.44 (m, 2H, H_2CN), 3.81 (m, 2H, H_2CN), 6.88−7.39 (m, *H*Ar), 7.49 (m, 2H, *H*C=N). ^{13}C {^{1}H} NMR (100 MHz, CD_2Cl_2) δ: 26.4 (d, J_{CP} = 11.0 Hz, C_{Cy}P), 27.8 (m, C_{Cy}P), 29.5 (t, J_{CP} = 3.4 Hz, C_{Cy}P), 30.2 (C_{Cy}P), 30.8 (d, J_{CP} = 8.7 Hz, C_{Cy}P), 38.3 (q, J_{CP} = 7.8 Hz, C_{Cy}P), 39.7 (dd, J_{CP} = 11.7, 16.9 Hz, C_{Cy}P), 60.9 (CH_2N), 122.7 (C_{Ph}B), 126.5 (C_{Ph}B), 136.7 (C_{Ph}B), 164.7 (m, J_{CB} = 49 Hz, C_{Ph}B), 174.4 (H*C*=N). ^{31}P {^{1}H} NMR (161 MHz, CD_2Cl_2) δ: 69.8 ppm. IR (KBr) 1948 cm^{-1} ($\nu_{C\equiv O}$). Anal. Calcd for $C_{55}H_{74}N_2OP_2FeBrB$: C, 66.88; H, 7.55; N, 2.84; Found: C, 65.30; H, 7.89; N, 3.15. MS (ESI, methanol/water; m/z^+): 667.2 $[C_{31}H_{53}N_2OP_2FeBr]^+$.

***trans*-(*S,S*)-[Fe(CO)(Br)(PCy$_2$CH$_2$CH=NCH(Ph)CH(Ph)N=CHCH$_2$PCy$_2$)][BPh$_4$] ((*S,S*)-11).** A solution of (1*S*,2*S*)-(-)-1,2-diphenylethylenediamine (33 mg, 0.156 mmol) in CH_3CN (1 mL) was added to precursor solution **A**. Thereafter the mixture was handled in the exact same manner as **10.** Yield: 66% (118 mg). ^{1}H NMR (400 MHz, CD_3CN) δ: 1.35−1.93 (br. m, *H*Cy), 2.48 (m, 1H, *H*C$_{Cy}$P), 2.81 (br. m, 2H, H_2CP, *H*C$_{Cy}$P), 3.04 (br. m, 2H, H_2CP), 3.54 (m, 1H, H_2CP), 4.99 (d, 1H, J_{HH} = 10.9 Hz, *H*CPh), 5.55 (d, 1H, J_{HH} = 11.7 Hz, *H*CPh), 6.86−7.50 (br. m, *H*Ar, *H*C=N), 7.88 (m, 2H, *H*C=N). ^{13}C {^{1}H} NMR (100 MHz, CD_3CN) δ: 26.7−40.5 (C_{Cy}P, CH_2P), 77.2 (*C*HPh), 80.3 (*C*HPh), 121.1 (C_{Ph}B), 124.9 (C_{Ph}B), 128.3 (C_{Ph}), 128.5 (C_{Ph}), 128.8 (C_{Ph}), 128.9 (C_{Ph}), 129.0 (C_{Ph}), 129.1 (C_{Ph}), 131.6 (C_{Ph}), 132.2 (C_{Ph}), 135.0 (C_{Ph}B), 162.6 (m, J_{CB} = 49 Hz), 172.0 (H*C*=N), 172.4 (H*C*=N). ^{31}P {^{1}H} NMR (161 MHz, CD_3CN) δ: 67.1 (d, J_{PP} = 29.8 Hz), 70.4 (d, J_{PP} = 29.8 Hz). IR (KBr) 1945 cm^{-1} ($\nu_{C\equiv O}$). Anal. Calcd for $C_{67}H_{82}N_2OP_2FeBrB$: C, 70.60; H, 7.25; N, 2.46. Found: C, 68.09; H, 7.03; N, 2.62. MS (ESI, methanol/water; m/z^+): 819.3 $[C_{43}H_{62}N_2OP_2FeBr]^+$.

***trans*-[Fe(NCMe)$_2$(P*i*Pr$_2$PCH$_2$CH=NCH$_2$CH$_2$N=CHCH$_2$-P*i*Pr$_2$)][BPh$_4$]$_2$ (7).** A vial was charged with **6** (50 mg, 0.104 mmol), KO*t*Bu (24 mg, 0.207 mmol), and CH_3CN (2 mL). After stirring for 5 min, $[Fe(H_2O)_6][BF_4]_2$ (52 mg, 0.156 mmol) in CH_3CN (1 mL) was added to the white slurry. The solution turned gray-yellow after 5 min. To this mixture, ethylenediamine (0.12 mL from a stock solution of 200 mg in 4 mL of CH_3CN) was added. After the reaction stirred overnight, the pink mixture was filtered through a pad of Celite. The solvent was removed under reduced pressure, taken up in MeOH (1.5 mL), and added to $NaBPh_4$ (78 mg, 0.228 mmol) in MeOH (1 mL) to cause the precipitation of a pale pink solid. The solid was filtered and washed with MeOH (2 × 1 mL) and dried under vacuum. Yield: 65% (75 mg). Single crystals suitable for an X-ray diffraction study were obtained by slow diffusion of hexanes into a 1:1 solution of THF and MeCN. ^{1}H NMR (400 MHz, CD_3CN) δ: 1.23 (m, 24H, CH(CH_3)$_2$), 1.98 (s, NCCH_3), 2.35 (m, 4H, C*H*(CH$_3$)$_2$), 3.35 (d, J_{HP} = 7.00 Hz, CH_2P), 4.00 (s, 4H, CH_2N), 6.87−7.30 (m, 40H, *H*Ar), 8.50 (m, 2H, *H*C=N). ^{13}C {^{1}H} NMR (100 MHz, CD_3CN) δ: 18.8 (d, J_{CP} = 6.6 Hz, CH(*C*H$_3$)$_2$), 24.8 (dd, J_{CP} = 7.2, 8.7 Hz, *C*H(CH$_3$)$_2$), 37.0 (dd, J_{CP} = 9.9, 14.6 Hz, *C*H$_2$P), 60.6 (*C*H$_2$N), 122.2 (C_{Ar}B), 126.0 (C_{Ar}B), 136.2 (C_{Ar}B), 164.2 (m, J_{CB} = 49.0 Hz, C_{Ar}B), 177.6 (H*C*=N). ^{31}P {^{1}H} NMR (161 MHz, CD_2Cl_2) δ: 75.9 (s) ppm.

Precursor Solution B. A vial was charged with **6** (100 mg, 0.207 mmol), KO*t*Bu (47 mg, 0.415 mmol), and CH_3CN (4 mL). After stirring for 5 min, $[Fe(H_2O)_6][BF_4]_2$ (105 mg, 0.311 mmol) in CH_3CN (2 mL) was added to the white slurry. The solution turned gray-yellow after 5 min.

***trans*-[Fe(CO)(Br)(P*i*Pr$_2$CH$_2$CH=NCH$_2$CH$_2$N=CHCH$_2$-P*i*Pr$_2$)][BPh$_4$] (12).** To precursor solution **B**, ethylenediamine (0.22 mL from a stock solution of 200 mg in 4 mL of CH_3CN) was added. The mixture turned pink immediately. After the reaction has gone to completion overnight, the mixture was filtered through a pad of Celite to remove a gray-white precipitate. Solvent was removed under reduced pressure to give a red-pink residue, which was then dissolved in acetone (6 mL) and stirred overnight under CO (∼2 atm). Acetone solvent was removed under pressure, taken up in MeOH (1.5 mL) and added to a solution of $NaBPh_4$ (106 mg, 0.311 mmol) in MeOH (1 mL) to cause precipitation of a yellow solid. The solid was filtered and washed with MeOH (2 × 1 mL) and dried under vacuum. Yield: 58% (100 mg). ^{1}H NMR (400 MHz, CD_2Cl_2) δ: 1.26 (m, 24H, CH_3), 2.28 (m, 2H, MeC*H*), 2.86 (m, 4H, MeC*H*, CH_2P), 3.24 (dd, J_{HH} = 7.9 Hz, J_{HP} = 25.2 Hz, 2H, CH_2P), 3.43 (m, 2H, CH_2N), 3.75 (m, 2H, CH_2N), 6.86−7.39 (m, 22H, *H*Ar, HC=N). ^{13}C {^{1}H} NMR (100 MHz, CD_2Cl_2) δ: 19.8 (*C*H$_3$), 20.0 (*C*H$_3$), 26.6 (t, J_{CP} = 8.9 Hz, *C*HMe$_2$), 27.5 (t, J_{CP} = 8.3 Hz, *C*HMe$_2$), 40.5 (dd, J_{CP} = 12.1, 16.6 Hz, *C*H$_2$P), 60.6 (*C*H$_2$N), 122.5 (C_{Ar}B), 126.3 (C_{Ar}B), 136.4 (C_{Ar}B), 164.5 (m, J_{CB} = 49 Hz, C_{Ar}B), 174.6 (H*C*=N). ^{31}P {^{1}H} NMR (161 MHz, CD_2Cl_2) δ: 77.7 (s) ppm. IR (KBr) 1948 cm^{-1} ($\nu_{C\equiv O}$). Anal. Calcd for $C_{43}H_{58}N_2OP_2FeBrB$: C, 62.42; H, 7.07; N, 3.39; Found: C, 64.45; H, 7.33; N, 3.90. MS (ESI, methanol/water; m/z^+): 507.1 $[C_{19}H_{38}N_2OP_2FeBr]^+$.

***trans*-(*S,S*)-[Fe(CO)(Br)(P*i*Pr$_2$CH$_2$CH=NCH(Ph)CH(Ph)N=CHCH$_2$P*i*Pr$_2$)][BPh$_4$] ((*S,S*)-13).** A solution of (1*S*,2*S*)-(-)-1,2-diphenylethylenediamine (44 mg, 0.207 mmol) in CH_3CN (1 mL) was added to precursor solution **B**. Thereafter the mixture was handled in the exact same manner as **12.** Yield: 60% (121 mg). Single crystals suitable for an X-ray diffraction study were obtained by slow diffusion of pentane into CH_2Cl_2. ^{1}H NMR (400 MHz, CD_3CN) δ: 1.32 (m, 24H, CCH_3), 2.35 (m, 2H, Me$_2$C*H*), 2.72 (m, 2H, Me$_2$C*H*), 3.03 (m, 3H, CH_2P), 3.59 (m, 2H, CH_2P), 5.06 (d, 1H, J_{HH} = 12 Hz, PhC*H*), 5.47 (d, 1H, J_{HH} = 12 Hz, PhC*H*), 6.87−7.55 (m, 32H, *H*Ar, *H*C=N). ^{13}C {^{1}H} NMR (100 MHz, CD_3CN) δ: 19.41 (Me), 19.45 (Me), 19.5 (Me), 19.8 (Me), 19.9 (Me), 20.3 (Me), 20.4 (Me), 20.6 (Me), 26.2 (d, J_{CP} = 18.9 Hz, Me*C*H), 26.9 (d, J_{CP} = 19.7 Hz, Me*C*H), 27.6 (d, J_{CP} = 20.1, Me*C*H), 29.1 (d, J_{CP} = 16.0 Hz, Me*C*H), 39.6 (dd, J_{CP} = 3.8, 23.2 Hz, *C*H$_2$P), 40.6 (dd, J_{CP} = 3.2, 25.3 Hz, *C*H$_2$P), 77.6 (Ph*C*H), 81.2 (Ph*C*H), 122.4 (C_{Ar}B), 126.2 (C_{Ar}B), 129.6 (C_{Ar}), 129.9 (C_{Ar}), 130.4 (C_{Ar}), 130.6 (C_{Ar}), 132.8 (C_{Ar}), 134.1 (C_{Ar}), 136.5 (C_{Ar}B), 164.5 (m, J_{CB} = 49.0 Hz, C_{Ar}B), 174.9 (H*C*=N), 175.0 (H*C*=N). ^{31}P {^{1}H} NMR (161 MHz, CD_3CN) δ: 67.1 (d, J_{PP} = 29.8 Hz), 70.4 (d, J_{PP} = 29.8 Hz). IR (KBr) 1956 cm^{-1} ($\nu_{C\equiv O}$). Anal. Calcd for $C_{55}H_{66}N_2OP_2FeBrB$: C, 67.43; H, 6.79; N, 2.86. Found: C, 70.96; H, 6.38; N, 2.19. MS (ESI, methanol/water; m/z^+): 661.2 $[C_{31}H_{47}N_2OP_2FeBr]^+$.

***trans*-[Fe(NCMe)$_2$(PEt$_2$CH$_2$CH=NCH$_2$CH$_2$N=CHCH$_2$-PEt$_2$)][BPh$_4$]$_2$ (9).** A vial was charged with **8** (60 mg, 0.141 mmol), KO*t*Bu (32 mg, 0.282 mmol), MeOH (5 mL). After stirring for 5 min, $[Fe(H_2O)_6][BF_4]_2$ (71 mg, 0.211 mmol) in CH_3CN (1 mL) was added to the white slurry the solution turned gray-yellow after 5 min. To this mixture, ethylenediamine (0.16 mL from a stock solution of 200 mg in 4 mL of CH_3CN) was added, and the reaction was refluxed overnight. The solvent was then removed, taken up in acetonitrile, and filtered through a pad of Celite to remove a gray-white precipitate. The solvent was then removed again taken up in MeOH (1 mL) and added to $NaBPh_4$ (105 mg, 0.310 mmol) in MeOH (1 mL) to cause precipitation of a pale pink solid. The solid was filtered and washed with MeOH (2 × 1 mL) and dried under vacuum. Yield: 70% (105 mg). Single crystals suitable for an X-ray diffraction study were obtained by slow diffusion of Et_2O into CH_2Cl_2. ^{1}H NMR (400 MHz, CD_3CN) δ: 1.13 (m, 12H, CH_3), 1.80 (m, CH_2CH$_3$), 3.41 (m, 4H, C*H*(CH$_3$)$_2$), 3.35 (d, J_{HP} = 7.74 Hz, CH_2P), 4.01 (s, 4H, CH_2N), 6.85−7.28 (m, 40H, *H*Ar), 8.41 (m, 2H, *H*C=N). ^{13}C {^{1}H} NMR (100 MHz, CD_3CN) δ: 9.9 (t, J_{CP} = 2.0 Hz, *C*H$_3$), 18.1 (dd, J_{CP} = 9.1, 11.4 Hz, *C*H(CH$_3$)$_2$), 41.8 (dd, J_{CP} = 11.4, 15.1 Hz, *C*H$_2$P), 61.4 (*C*H$_2$N), 122.6 (C_{Ar}B), 126.3 (C_{Ar}B), 136.2 (C_{Ar}B), 163.9 (m, J_{CB} = 49.0 Hz, C_{Ar}B), 175.4 (H*C*=N). ^{31}P {^{1}H} NMR (161 MHz, CD_2Cl_2) δ: 70.5 (s) ppm.

Precursor Solution C. A vial was charged with **8** (150 mg, 0.352 mmol), KO*t*Bu (79 mg, 0.704 mmol), and MeOH (5 mL). After stirring for 5 min, $[Fe(H_2O)_6][BF_4]_2$ (178 mg, 0.528 mmol)

in CH_3CN (2 mL) was added to the white slurry. The solution turned gray-yellow after 5 min.

***trans*-[Fe(CO)(Br)(PEt_2CH_2CH=NCH_2CH_2N=$CHCH_2PEt_2$)][BPh_4] (14).** To precursor solution **C**, ethylenediamine (0.38 mL from a stock solution of 200 mg in 4 mL of CH_3CN) was added. The mixture turned red immediately and was allowed to reflux overnight (the reaction mixture turned to a pale orange-yellow color). The solvent was removed, the residue was taken up with acetonitrile, and filtered through a pad of Celite to remove a gray-white precipitate. The acetonitrile solvent was removed under reduced pressure to give a pale-pink residue, which was then dissolved in acetone (6 mL) and stirred overnight under CO (~ 2 atm). Acetone solvent was removed under pressure, taken up in MeOH (2 mL), and added to a solution of $NaBPh_4$ (180 mg, 0.528 mmol) in MeOH (1.5 mL) to cause precipitation of a yellow solid. The solid was filtered and washed with MeOH (2 × 1 mL) and dried under vacuum. Yield: 55% (150 mg). Single crystals suitable for an X-ray diffraction study were obtained by slow diffusion of hexanes into CH_2Cl_2. ^{1}H NMR (400 MHz, CD_2Cl_2) δ: 1.10 (m, 12H, CH_3), 1.89 (m, 6H, CH_2CH$_3$), 2.90 (dd, 2H, J_{HH} = 7.01 Hz, J_{HP} = 19.20, CH_2P), 3.19 (dd, 2H, J_{HH} = 7.63 Hz, J_{HP} = 19.2 Hz, CH_2P), 3.58 (m, 2H, CH_2N), 3.76 (m, 2H, CH_2N), 6.89−7.35 (m, 22H, *H*Ar, *H*C=N). ^{13}C {^{1}H} NMR (100 MHz, CD_2Cl_2) δ: 8.08 (Me), 8.26 (Me), 17.9 (t, J_{CP} = 11.8 Hz, *C*H$_2$Me), 19.9 (t, J_{CP} = 12.7 Hz, *C*H$_2$Me), 41.3 (dd, J_{CP} = 13.5, 16.8 Hz, *C*H$_2$P), 59.8 (*C*H$_2$N), 122.3 (C_{Ar}B), 126.1 (C_{Ar}B), 136.1 (C_{Ar}B), 164.2 (m, J_{CB} = 49 Hz, C_{Ar}B), 173.2 (H*C*=N). ^{31}P {^{1}H} NMR (161 MHz, CD_2Cl_2) δ: 66.8 ppm. IR (KBr) 1951 cm^{-1} ($\nu_{C\equiv O}$). Anal. Calcd for $C_{39}H_{50}N_2OP_2FeBrB$: C, 60.73; H, 6.53; N, 3.63; Found: C, 58.16; H, 6.26; N, 3.40. MS (ESI, methanol/water; m/z^+): 451.0 $[C_{15}H_{30}N_2OP_2FeBr]^+$.

***trans*-(*S*,*S*)-[Fe(CO)(Br)(PEt_2CH_2CH=NCH(Ph)CH(Ph)N=$CHCH_2PEt_2$)][BPh_4] ((*S*,*S*)-15).** A solution of (1*S*,2*S*)-(-)-1,2-diphenylethylenediamine (75 mg, 0.352 mmol) in CH_3CN (1 mL) was added to precursor solution **C**. Thereafter the mixture was handled in the exact same manner as **14**. An extra purification step is required, as the product does not precipitate effectively from methanol (an appreciable amount remains dissolved in methanol). The methanol solution was concentrated to a residue, taken up with CH_2Cl_2 (1 mL), and filtered to remove excess $NaBPh_4$. Et_2O (15 mL) was added to cause precipitation. Yield: 84% (275 mg). Single crystals suitable for an X-ray diffraction study were obtained by slow diffusion of hexanes into CH_2Cl_2. ^{1}H NMR (400 MHz, CD_3CN) δ: 1.18 (m, 12H, CH_3), 1.94 (m, 4H, CH_2CH$_3$), 2.42 (m, 2H, CH_2CH$_3$) 2.64 (m, 2H, CH_2CH$_3$), 2.98 (m, 3H, CH_2P), 3.42 (m, 1H, CH_2P), 5.13 (d, 1H, J_{HH} = 11.4 Hz, C*H*(Ph)), 5.37 (d, 1H, J_{HH} = 11.4 Hz, C*H*(Ph)), 6.84−7.32 (m, 32H, *H*Ar, *H*C=N). ^{13}C {^{1}H} NMR (100 MHz, CD_3CN) δ: ^{13}C {^{1}H} NMR (100 MHz, CD_3CN) δ: 8.11 (*C*H$_3$), 8.17 (*C*H$_3$), 8.50 (*C*H$_3$), 8.58 (*C*H$_3$), 8.78 (*C*H$_3$), 17.7 (d, J_{CP} = 26.2 Hz, *C*H$_2$CH$_3$), 19.2 (d, J_{CP} = 24.0 Hz, *C*H$_2$CH$_3$), 20.4 (d, J_{CP} = 27.6 Hz, *C*H$_2$CH$_3$), 20.6 (d, J_{CP} = 25.6 Hz, *C*H$_2$CH$_3$), 77.8 (*C*H(Ph)), 81.7 (*C*H(Ph)), 122.3 (C_{Ar}B), 126.2 (C_{Ar}B), 127.5 (C_{Ar}), 128.7 (C_{Ar}), 129.4 (C_{Ar}), 129.7 (C_{Ar}), 130.0 (C_{Ar}), 130.1 (C_{Ar}), 130.2 (C_{Ar}), 130.4 (C_{Ar}), 132.9 (C_{Ar}), 134.5 (C_{Ar}), 136.3 (C_{Ar}B), 164.4 (m, J_{CB} = 49 Hz, C_{Ar}B), 173.4 (H*C*=N), 174.2 (H*C*=N). ^{31}P {^{1}H} NMR (161 MHz, CD_3CN) δ: 66.8 (d, J_{PP} = 34.3 Hz), 67.9 (d, J_{PP} = 34.3 Hz). IR (KBr) 1951 cm^{-1} ($\nu_{C\equiv O}$). Anal. Calcd for $C_{51}H_{59}N_2OP_2FeBrB$: C, 66.25; H, 6.43; N, 3.03. Found: C, 66.81; H, 6.29; N, 2.81. MS (ESI, methanol/water; m/z^+): 603.1 $[C_{27}H_{38}N_2OP_2FeBr]^+$.

General Procedure for Transfer Hydrogenation Studies. A solution of potassium *tert*-butoxide (10 mg, 0.089 mmol) in *iso*-propanol (4 mL) was added via syringe to a Schlenk flask charged with a mixture of (*S*,*S*)-**15** (10 mg, 0.011 mmol), acetophenone (651 mg, 5.418 mmol) in 2 mL of *iso*-propanol at 50 °C under an atmosphere of argon. Samples were taken from the reaction mixture periodically via a syringe and needle and were quenched upon exposure to air. The samples were analyzed by gas chromatography (GC) using a Perkin-Elmer Clarus 400 chromatograph equipped with a chiral column (CP chirasil-Dex CB 25 m × 2.5 mm). Hydrogen was used as a mobile phase at a column pressure of 5 psi with a split flow rate of 50 mL/min. The injector temperature was 250 °C, FID temperature was 275 °C, and the oven temperature was 130 °C. Retention times (t_R/min) for acetophenone, 4.33; (*R*)-1-phenylethanol, 7.17; (*S*)-1-phenylethanol, 7.67. All conversions were reported as an average of two GC runs.

Acknowledgment. We thank NSERC Canada for a Discovery grant to R.H.M.

Supporting Information Available: Complete crystallographic data in CIF format for complexes **7**, **9**·CH_2Cl_2, **10**·**THF**, (*S*,*S*)-**13**, **14**, and (*S*,*S*)-**15**. This material is available free of charge via the Internet at http://pubs.acs.org.